

Photoluminescent Properties of Chalcobromide-capped Octahedral Hexarhenium(III) Complexes $[\{\text{Re}_6\text{Q}_{8-n}\text{Br}_n\}\text{Br}_6]^{n-4}$ (Q = Se, $n = 1-3$; Q = S, $n = 1, 2$)

Takashi Yoshimura,^{*,†} Ayumi Matsuda,[†] Yuki Ito,[‡] Shoji Ishizaka,[‡] Satoshi Shinoda,[§] Hiroshi Tsukube,[§] Noboru Kitamura,[‡] and Atsushi Shinohara[†]

[†]Department of Chemistry, Graduate School of Science, Osaka University, Toyonaka 560-0043, Japan,

[‡]Department of Chemistry, Graduate School of Science, Hokkaido University, Sapporo 060-0810, Japan, and

[§]Department of Chemistry, Graduate School of Science, and CREST, Japan Science and Technology Corporation (JST), Osaka City University, Osaka 558-8585, Japan

Received December 28, 2009

Photoluminescent properties of chalcobromide-capped octahedral hexarhenium(III) complexes with terminal bromide ligands $[\{\text{Re}_6\text{Q}_{8-n}\text{Br}_n\}\text{Br}_6]^{n-4}$ (Q = Se, $n = 1$ ($[\text{1-Se}]^{3-}$), $n = 2$ ($[\text{2a-Se}]^{2-}$ and $[\text{2b-Se}]^{2-}$), and $n = 3$ ($[\text{3-Se}]^{-}$); Q = S, $n = 1$ ($[\text{1-S}]^{3-}$), $n = 2$ ($[\text{2a-S}]^{2-}$, $[\text{2b-S}]^{2-}$, and $[\text{2c-S}]^{2-}$) were studied. The Q-Br capped complex $[\{\text{Re}_6\text{Q}_7\text{Br}\}\text{Br}_6]^{3-}$ and Q_6Br_2 $[\{\text{Re}_6\text{Q}_6\text{Br}_2\}\text{Br}_6]^{2-}$ (both D_{3d} and C_{2v} symmetric geometrical isomers) were successfully separated by column chromatography. All of the chalcobromide-capped complexes studied showed photoluminescence in both crystalline and solution phases. The emission maximum wavelength of the complexes at 296 K spans 853–915 or 868–968 nm in the crystalline phase or in acetonitrile, respectively. The selenobromide-capped complexes showed more intense emission as compared with the thiobromide analogues. The emission quantum yield (Φ_{em}) and emission lifetime (τ_{em}) became smaller and shorter, respectively, with an increase in the number of a capping bromide ligand in $[\{\text{Re}_6\text{Q}_{8-n}\text{Br}_n\}\text{Br}_6]^{n-4}$. In the crystalline phase at 80 K, the emission maximum of the chalcobromide-capped complex shifted to the longer wavelength relative to that at 296 K. The emissive excited-state of the chalcobromide-capped hexarhenium(III) complexes was concluded to originate from the $\{\text{Re}_6\text{Q}_{8-n}\text{Br}_n\}^{n+2}$ core with a spin-triplet type. The Φ_{em} and τ_{em} values of the $\{\text{Re}_6\text{Q}_{8-n}\text{Br}_n\}^{n+2}$ complex were dependent significantly on the symmetry of the hexarhenium core, showing more intense emission for the complex with the higher symmetric core. A linear correlation between natural logarithm of the nonradiative decay rate constant and the emission maximum energy was observed for $[\{\text{Re}_6\text{Q}_6\text{Br}_2\}\text{Br}_6]^{2-}$.

Introduction

The octahedral hexanuclear complexes having 24 valence electrons with the $\{\text{Re}_6\text{Q}_8\}^{2+}$ (Q = S, Se, or Te) or $\{\text{M}_6\text{X}_8\}^{4+}$

(M = Mo(II) or W(II), X = Cl, Br, or I) core show photoluminescence in visible and near-infrared regions.^{1–32} The photophysical properties of these complexes have been

*To whom correspondence should be addressed. E-mail: tyoshi@chem.sci.osaka-u.ac.jp. Phone: 81-6-6850-5416. Fax: 81-6-6850-5418.

(1) Gray, T. G.; Rudzinski, C. M.; Nocera, D. G.; Holm, R. H. *Inorg. Chem.* **1999**, *38*, 5932–5933.

(2) Guilbaud, C.; Deluzet, A.; Domercq, B.; Molinie, P.; Boubekeur, K.; Batail, P.; Coulon, C. *Chem. Commun.* **1999**, 1867–1868.

(3) Yoshimura, T.; Ishizaka, S.; Umakoshi, K.; Sasaki, Y.; Kim, H.-B.; Kitamura, N. *Chem. Lett.* **1999**, 697–698.

(4) Yoshimura, T.; Ishizaka, S.; Sasaki, Y.; Kim, H.-B.; Kitamura, N.; Naumov, N. G.; Sokolov, M. N.; Fedorov, V. E. *Chem. Lett.* **1999**, 1121–1122.

(5) Yoshimura, T.; Umakoshi, K.; Sasaki, Y.; Ishizaka, S.; Kim, H.-B.; Kitamura, N. *Inorg. Chem.* **2000**, *39*, 1765–1772.

(6) Chen, Z.-N.; Yoshimura, T.; Abe, M.; Tsuge, K.; Sasaki, Y.; Ishizaka, S.; Kim, H.-B.; Kitamura, N. *Chem.—Eur. J.* **2001**, *7*, 4447–4455.

(7) Gabriel, J.-C. P.; Boubekeur, K.; Uriel, S.; Batail, P. *Chem. Rev.* **2001**, *101*, 2037–2066.

(8) Gray, T. G.; Rudzinski, C. M.; Meyer, E. E.; Holm, R. H.; Nocera, D. G. *J. Am. Chem. Soc.* **2003**, *125*, 4755–4770.

(9) Yoshimura, T.; Chen, Z.-N.; Itasaka, A.; Abe, M.; Sasaki, Y.; Ishizaka, S.; Kitamura, N.; Yarovoi, S. S.; Solodovnikov, S. F.; Fedorov, V. E. *Inorg. Chem.* **2003**, *42*, 4857–4863.

(10) Gray, T. G.; Rudzinski, C. M.; Meyer, E. E.; Nocera, D. G. *J. Phys. Chem. A* **2004**, *108*, 3238–3243.

(11) Kitamura, N.; Ueda, Y.; Ishizaka, S.; Yamada, K.; Aniya, M.; Sasaki, Y. *Inorg. Chem.* **2005**, *44*, 6308–6313.

(12) Mironov, Y. V.; Brylev, K. A.; Shestopalov, M. A.; Yarovoi, S. S.; Fedorov, V. E.; Spies, H.; Pietzsch, H.-J.; Stephan, H.; Geipel, G.; Bernhard, G.; Kraus, W. *Inorg. Chim. Acta* **2006**, *359*, 1129–1134.

(13) Brylev, K. A.; Mironov, Y. V.; Yarovoi, S. S.; Naumov, N. G.; Fedorov, V. E.; Kim, S.-J.; Kitamura, N.; Kuwahara, Y.; Yamada, K.; Ishizaka, S.; Sasaki, Y. *Inorg. Chem.* **2007**, *46*, 7414–7422.

(14) Kim, S.; Kim, Y.; Lee, J.; Shin, W.; Lee, M.; Kim, S.-J. *Inorg. Chim. Acta* **2007**, *360*, 1890–1894.

(15) Brylev, K. A.; Mironov, Y. V.; Kozlova, S. G.; Fedorov, V. E.; Kim, S.-J.; Pietzsch, H.-J.; Stephan, H.; Ito, A.; Ishizaka, S.; Kitamura, N. *Inorg. Chem.* **2009**, *48*, 2309–2315.

(16) Dorson, F.; Molard, Y.; Cordier, S.; Fabre, B.; Efremova, O.; Rondeau, D.; Mironov, Y.; Circu, V.; Naumov, N.; Perrin, C. *Dalton Trans.* **2009**, 1297–1299.

(17) Kim, Y.; Fedorov, V. E.; Kim, S.-J. *J. Mater. Chem.* **2009**, *19*, 7178–7190.

(18) Gray, T. G. *Chem.—Eur. J.* **2009**, *15*, 2581–2593.

(19) Gray, H. B.; Maverick, A. W. *Science* **1981**, *214*, 1201–1205.

(20) Maverick, A. W.; Gray, H. B. *J. Am. Chem. Soc.* **1981**, *103*, 1298–1300.

(21) Maverick, A. W.; Najdzionek, J. S.; MacKenzie, D.; Nocera, D. G.; Gray, H. B. *J. Am. Chem. Soc.* **1983**, *105*, 1878–1882.

studied extensively by both experiments and theoretical calculations.^{1–38} It has been found that luminescence of these complexes originates from the spin-triplet excited-state localized on the hexanuclear core. A number of chalcogenide-capped hexanuclear complexes with a $\{\text{Re}_6\text{Q}_{8-n}\text{X}_n\}^{n+2}$ (Q = S, Se; X = Cl, Br; $n = 1-4$) or $\{\text{Mo}_6\text{Q}_{8-n}\text{X}_n\}^{n-4}$ (Q = S, Se; X = Cl, Br; $n = 7$ or 6) core have been synthesized and their

properties have been investigated.^{7,30,39–96} However, photoluminescence of chalcogenide-capped complexes have been reported only for *fac*- $[\{\text{Re}_6\text{Q}_7\text{Br}\}\text{Br}_3(\text{EPh}_3)_3]$ (Q = S, Se;

- (22) Nocera, D. G.; Gray, H. B. *J. Am. Chem. Soc.* **1984**, *106*, 824–825.
 (23) Saito, Y.; Tanaka, H. K.; Sasaki, Y.; Azumi, T. *J. Phys. Chem.* **1985**, *89*, 4413–4415.
 (24) Zietlow, T. C.; Hopkins, M. D.; Gray, H. B. *J. Solid State Chem.* **1985**, *57*, 112–119.
 (25) Zietlow, T. C.; Nocera, D. G.; Gray, H. B. *Inorg. Chem.* **1986**, *25*, 1351–1353.
 (26) Zietlow, T. C.; Schaefer, W. P.; Sadeghi, B.; Hua, N.; Gray, H. B. *Inorg. Chem.* **1986**, *25*, 2195–2198.
 (27) Azumi, T.; Saito, Y. *J. Phys. Chem.* **1988**, *92*, 1715–1721.
 (28) Tanaka, H. K.; Sasaki, Y.; Ebihara, M.; Saito, K. *Inorg. Chim. Acta* **1989**, *161*, 63–66.
 (29) Miki, H.; Ikeyama, T.; Sasaki, Y.; Azumi, T. *J. Phys. Chem.* **1992**, *96*, 3236–3239.
 (30) Kozhomuratova, Z. S.; Mironov, Y. V.; Shestopalov, M. A.; Drebushchak, I. V.; Moroz, N. K.; Naumov, D. Y.; Smolentsev, A. I.; Uskov, E. M.; Fedorov, V. E. *Eur. J. Inorg. Chem.* **2007**, 2055–2060.
 (31) Szczepura, L. F.; Ketcham, K. A.; Ooro, B. A.; Edwards, J. A.; Templeton, J. N.; Cedeno, D. L.; Jircitano, A. J. *Inorg. Chem.* **2008**, *47*, 7271–7278.
 (32) Szczepura, L. F.; Edwards, J. A.; Cedeno, D. L. *J. Cluster Sci.* **2009**, *20*, 105–112.
 (33) Arratia-Perez, R.; Hernandez-Acevedo, L. *J. Chem. Phys.* **1999**, *111*, 168–172.
 (34) Arratia-Perez, R.; Hernandez-Acevedo, L. *J. Chem. Phys.* **1999**, *110*, 2529–2532.
 (35) Honda, H.; Noro, T.; Tanaka, K.; Miyoshi, E. *J. Chem. Phys.* **2001**, *114*, 10791–10797.
 (36) Kozlova, S. G.; Gabuda, S. P.; Brylev, K. A.; Mironov, Y. V.; Fedorov, V. E. *J. Phys. Chem. A* **2004**, *108*, 10565–10567.
 (37) Roy, L. E.; Hughbanks, T. *Inorg. Chem.* **2006**, *45*, 8273–8282.
 (38) Ramirez-Tagle, R.; Arratia-Perez, R. *Chem. Phys. Lett.* **2008**, *455*, 38–41.
 (39) Fedorov, V. E.; Mishchenko, A. V.; Kolesov, B. A.; Gubin, S. P.; Slovokhotov, Y. L.; Struchkov, Y. T. *Izv. Akad. Nauk SSSR, Ser. Khim.* **1984**, 2159–2160.
 (40) Pilet, J. C.; Le Traon, F.; Le Traon, A.; Perrin, C.; Perrin, A.; Leduc, L.; Sergent, M. *Surf. Sci.* **1985**, *156*, 359–369.
 (41) Batail, P.; Ouahab, L.; Penicaud, A.; Lenoir, C.; Perrin, A. *C. R. Acad. Sci., Ser. 2* **1987**, *304*, 1111–1116.
 (42) Perrin, A.; Perrin, C.; Sergent, M. *J. Less-Common Met.* **1988**, *137*, 241–265.
 (43) Perrin, A.; Sergent, M. *New J. Chem.* **1988**, *12*, 337–356.
 (44) Renault, A.; Pouget, J. P.; Parkin, S. S. P.; Torrance, J. B.; Ouahab, L.; Batail, P. *Mol. Cryst. Liq. Cryst.* **1988**, *161*, 329–334.
 (45) Penicaud, A.; Lenoir, C.; Batail, P.; Coulon, C.; Perrin, A. *Synth. Met.* **1989**, *32*, 25–32.
 (46) Perrin, A. *New J. Chem.* **1990**, *14*, 561–567.
 (47) Perrin, A.; Leduc, L.; Potel, M.; Sergent, M. *Mater. Res. Bull.* **1990**, *25*, 1227–1234.
 (48) Perrin, A.; Leduc, L.; Sergent, M. *Eur. J. Solid State Inorg. Chem.* **1991**, *28*, 919–931.
 (49) Slougui, A.; Perrin, A.; Sergent, M. *Acta Crystallogr., Sect. C: Cryst. Struct. Commun.* **1992**, *C48*, 1917–1920.
 (50) Yaghi, O. M.; Scott, M. J.; Holm, R. H. *Inorg. Chem.* **1992**, *31*, 4778–4784.
 (51) Gabriel, J. C.; Boubekeur, K.; Batail, P. *Inorg. Chem.* **1993**, *32*, 2894–2900.
 (52) Penicaud, A.; Boubekeur, K.; Batail, P.; Canadell, E.; Auban-Senzier, P.; Jerome, D. *J. Am. Chem. Soc.* **1993**, *115*, 4101–4112.
 (53) Renault, A.; Lajzerowicz, J.; Batail, P.; Coulon, C. *Bull. Soc. Chim. Fr.* **1993**, *130*, 740–744.
 (54) Aruchamy, A.; Tamaoki, H.; Fujishima, A.; Berger, H.; Speziali, N. L.; Levy, F. *Mater. Res. Bull.* **1994**, *29*, 359–368.
 (55) Dolbecq, A.; Boubekeur, K.; Batail, P.; Canadell, E.; Auban-Senzier, P.; Coulon, C.; Lerstrup, K.; Bechgaard, K. *J. Mater. Chem.* **1995**, *5*, 1707–1718.
 (56) Uriel, S.; Boubekeur, K.; Batail, P.; Orduna, J.; Canadell, E. *Inorg. Chem.* **1995**, *34*, 5307–5313.
 (57) Dolbecq, A.; Fourmigue, M.; Batail, P. *Bull. Soc. Chim. Fr.* **1996**, *133*, 83–88.
 (58) Fedin, V. P.; Imoto, H.; Saito, T.; Fedorov, V. E.; Mironov, Y. V.; Yarovoi, S. S. *Polyhedron* **1996**, *15*, 1229–1233.
 (59) Uriel, S.; Boubekeur, K.; Gabriel, J.-C.; Batail, P.; Orduna, J. *Bull. Soc. Chim. Fr.* **1996**, *133*, 783–794.
 (60) Perrin, C. *J. Alloys Compd.* **1997**, *262–263*, 10–21.
 (61) Pinheiro, C. B.; Speziali, N. L.; Berger, H. *Acta Crystallogr., Sect. C: Cryst. Struct. Commun.* **1997**, *C53*, 1178–1180.
 (62) Slougui, A.; Ferron, S.; Perrin, A.; Sergent, M. *J. Cluster Sci.* **1997**, *8*, 349–359.
 (63) Yarovoi, S. S.; Mironov, Y. I.; Mironov, Y. V.; Virovets, A. V.; Fedorov, V. E.; Paek, U. H.; Shin, S. C.; Seo, M.-L. *Mater. Res. Bull.* **1997**, *32*, 1271–1277.
 (64) Guilbaud, C. B.; Gabriel, J.-C. P.; Boubekeur, K.; Batail, P. *C. R. Acad. Sci., Ser. II: Chim.* **1998**, *1*, 765–770.
 (65) Simon, F.; Boubekeur, K.; Gabriel, J.-C. P.; Batail, P. *Chem. Commun.* **1998**, 845–846.
 (66) Mironov, Y. V.; Fedorov, V. E.; Pell, M. A.; Ibers, J. A. *J. Struct. Chem.* **1999**, *39*, 609–614.
 (67) Perricone, A.; Slougui, A.; Perrin, A. *Solid State Sci.* **1999**, *1*, 657–666.
 (68) Saito, T. *J. Chem. Soc., Dalton Trans.* **1999**, 97–106.
 (69) Slougui, A.; Perrin, A.; Sergent, M. *J. Solid State Chem.* **1999**, *147*, 358–365.
 (70) Yarovoi, S. S.; Mironov, Y. V.; Solodovnikov, S. F.; Virovets, A. V.; Fedorov, V. E. *Mater. Res. Bull.* **1999**, *34*, 1345–1351.
 (71) Deluzet, A.; Batail, P.; Misaki, Y.; Auban-Senzier, P.; Canadell, E. *Adv. Mater.* **2000**, *12*, 436–439.
 (72) Solodovnikov, S. F.; Mironov, Y. V.; Yarovoi, S. S.; Virovets, A. V.; Fedorov, V. E. *Khim. Interesakh Ustoich. Razvit.* **2000**, *8*, 285–290.
 (73) Uriel, S.; Boubekeur, K.; Batail, P.; Orduna, J.; Perrin, A. *New J. Chem.* **2001**, *25*, 737–740.
 (74) Mironov, Y. V.; Naumov, N. G.; Yarovoi, S. S.; Cordier, S.; Perrin, C.; Fedorov, V. E. *Russ. Chem. Bull.* **2002**, *51*, 1919–1923.
 (75) Gray, T. G. *Coord. Chem. Rev.* **2003**, *243*, 213–235.
 (76) Pilet, G.; Cordier, S.; Perrin, C.; Perrin, A. *Inorg. Chim. Acta* **2003**, *350*, 537–546.
 (77) Yarovoi, S. S.; Solodovnikov, S. F.; Tkachev, S. V.; Mironov, Y. V.; Fedorov, V. E. *Russ. Chem. Bull.* **2003**, *52*, 68–72.
 (78) Solodovnikov, S. F.; Yarovoi, S. S.; Mironov, Y. V.; Vironets, A. V.; Fedorov, V. E. *J. Struct. Chem.* **2004**, *45*, 865–873.
 (79) Mironov, Y. V.; Ikorskii, V. N.; Fedorov, V. E.; Ibers, J. A. *Eur. J. Inorg. Chem.* **2005**, 214–217.
 (80) Perruchas, S.; Boubekeur, K.; Batail, P. *Cryst. Growth Des.* **2005**, *5*, 1585–1596.
 (81) Pilet, G.; Kirakci, K.; De Montigny, F.; Cordier, S.; Lapinte, C.; Perrin, C.; Perrin, A. *Eur. J. Inorg. Chem.* **2005**, 919–928.
 (82) Pilet, G.; Perrin, A. *C. R. Chim.* **2005**, *8*, 1728–1742.
 (83) Welch, E. J.; Long, J. R. In *Prog. Inorg. Chem.*; John Wiley & Sons, Inc, 2005; Vol. 54, pp 1–45.
 (84) Yarovoi, S. S.; Solodovnikov, S. F.; Solodovnikova, Z. A.; Mironov, Y. V.; Fedorov, V. E. *J. Struct. Chem.* **2006**, *47*, 97–101.
 (85) Yarovoi, S. S.; Mironov, Y. V.; Solodovnikov, S. F.; Solodovnikova, Z. A.; Naumov, D. Y.; Fedorov, V. E. *Russ. J. Coord. Chem.* **2006**, *32*, 712–722.
 (86) Shestopalov, M. A.; Mironov, Y. V.; Brylev, K. A.; Kozlova, S. G.; Fedorov, V. E.; Spies, H.; Pietzsch, H.-J.; Stephan, H.; Geipel, G.; Bernhard, G. *J. Am. Chem. Soc.* **2007**, *129*, 3714–3721.
 (87) Perruchas, S.; Boubekeur, K.; Canadell, E.; Misaki, Y.; Auban-Senzier, P.; Pasquier, C.; Batail, P. *J. Am. Chem. Soc.* **2008**, *130*, 3335–3348.
 (88) Shestopalov, M. A.; Mironov, Y. V.; Brylev, K. A.; Fedorov, V. E. *Russ. Chem. Bull.* **2008**, *57*, 1644–1649.
 (89) Fontaine, B.; Gautier, R.; Pilet, G.; Cordier, S.; Perrin, C.; Perrin, A.; Mironov, Y. V. *J. Cluster Sci.* **2009**, *20*, 145–151.
 (90) Shestopalov, M. A.; Cordier, S.; Hernandez, O.; Molard, Y.; Perrin, C.; Perrin, A.; Fedorov, V. E.; Mironov, Y. V. *Inorg. Chem.* **2009**, *48*, 1482–1489.
 (91) Perrin, C.; Sergent, M.; Le Traon, F.; Le Traon, A. *J. Solid State Chem.* **1978**, *25*, 197–204.
 (92) Michel, J. B.; McCarley, R. E. *Inorg. Chem.* **1982**, *21*, 1864–1872.
 (93) Ebihara, M.; Toriumi, K.; Saito, K. *Inorg. Chem.* **1988**, *27*, 13–18.
 (94) Ebihara, M.; Isobe, K.; Sasaki, Y.; Saito, K. *Inorg. Chem.* **1992**, *31*, 1644–1649.
 (95) Ebihara, M.; Toriumi, K.; Sasaki, Y.; Saito, K. *Gazz. Chim. Ital.* **1995**, *125*, 87–94.
 (96) Abramov, P. A.; Sokolov, M. N.; Virovets, A. V.; Peresypkina, E. V.; Vicent, C.; Fedin, V. P. *J. Cluster Sci.* **2009**, *20*, 83–92.

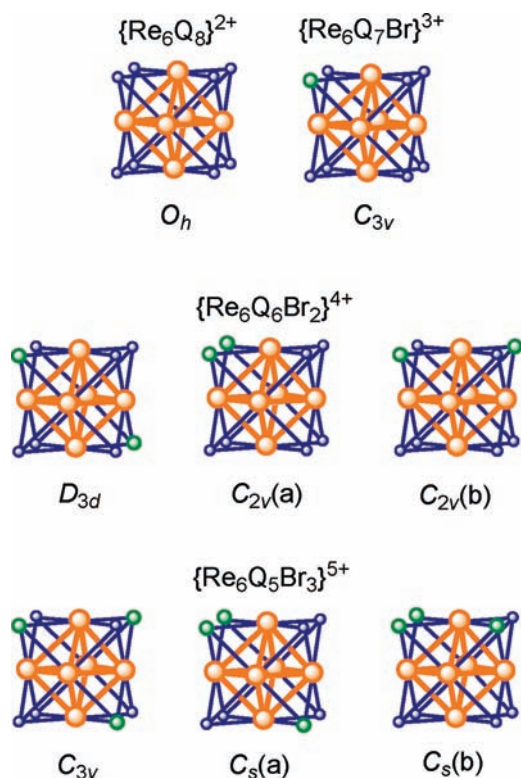


Figure 1. Structures and possible isomers of $\{\text{Re}_6\text{Q}_8\}^{2+}$, $\{\text{Re}_6\text{Q}_7\text{Br}\}^{3+}$, $\{\text{Re}_6\text{Q}_6\text{Br}_2\}^{4+}$, and $\{\text{Re}_6\text{Q}_5\text{Br}_3\}^{5+}$ cores (Q = S or Se).

E = P, As) and *fac*- $[\{\text{Re}_6\text{Q}_7\text{Br}\}\text{Br}_3(\text{pz})_3]$ at room temperature, where AsPh_3 , PPh_3 , and *pz* are triphenylarsine, triphenylphosphine, and pyrazine, respectively.^{86,88,90}

It is worth pointing out that a chalcobromide-capped octahedral hexanuclear complex possesses several geometrical isomers, depending on the number of a halide ligand in the $\{\text{Re}_6\text{Q}_{8-n}\text{Br}_n\}^{n+2}$ core (Q = S or Se) as shown in Figure 1. In the case of $\{\text{Re}_6\text{Q}_8\}^{2+}$ and $\{\text{Re}_6\text{Q}_7\text{Br}\}^{3+}$, the compounds possess only O_h and C_{3v} symmetrical complexes, respectively, while a set of the geometrical isomers is present in $\{\text{Re}_6\text{Q}_6\text{Br}_2\}^{4+}$ and $\{\text{Re}_6\text{Q}_5\text{Br}_3\}^{5+}$ as shown in Figure 1. Such geometrical isomers with different symmetrical structures might reflect on the spectroscopic and photophysical properties of the complexes, which are worth studying in detail for further advances in the research on hexanuclear complexes.

In the present study, the photoluminescent properties of a series of the chalcobromide-capped hexarhenium(III) complexes $[\{\text{Re}_6\text{Q}_{8-n}\text{Br}_n\}\text{Br}_6]^{n-4}$ (Q = Se, $n = 1-3$; Q = S, $n = 1, 2$) including the geometrical isomers of $[\{\text{Re}_6\text{Q}_6\text{Br}_2\}\text{Br}_6]^{2-}$ were investigated. It was found that the emission quantum yield (Φ_{em}) and emission lifetime (τ_{em}) of the complexes depended largely on both the number of a capping bromide ligand and the geometry of the $\{\text{Re}_6\text{Q}_{8-n}\text{Br}_n\}^{n+2}$ core. We report for the first time near-infrared ~ infrared emission of the hexarhenium complexes in both crystalline and solution phases, and demonstrate that the chalcobromide-capped hexarhenium complexes show the photoluminescence originating from the excited triplet state localized on the $\{\text{Re}_6\text{Q}_{8-n}\text{Br}_n\}^{n+2}$ core. In the case of $[\{\text{Re}_6\text{Q}_6\text{Br}_2\}\text{Br}_6]^{2-}$, furthermore, it is demonstrated that the photophysical data are dependent significantly on the geometrical structures.

Experimental Section

Materials. Spectroscopic grade acetonitrile (Wako) was used for photophysical measurements. All of other commercially available reagents were used as received.

Preparation of the Complexes. Separation of $(\text{Bu}_4\text{N})_{4-n}[\{\text{Re}_6\text{Se}_{8-n}\text{Br}_n\}\text{Br}_6]$ ($n = 1, 2$). The reported high temperature reaction method⁷⁷ was modified slightly to prepare the present hexarhenium(III) clusters. Elemental rhenium (400 mg, 2.15 mmol), selenium (170 mg, 2.15 mmol), cesium bromide (153 mg, 0.72 mmol), and bromine (55 μL , 1.07 mmol) were charged into a silica ampule (i.d. 8 mm \times o.d. 10 mm \times 10 cm), the ampule was evacuated thoroughly, and sealed under vacuum. The reactants were mixed and heated to 850 $^\circ\text{C}$ for 4.5 h, maintained at 850 $^\circ\text{C}$ for 67 h, and then cooled to room temperature during 3.5 h. The resultant solid was dissolved in water, and a large amount of the black residue was removed by filtration. An orange solid, precipitated upon an addition of tetra-*n*-butylammonium bromide (1.5 g, 4.7 mmol) to the filtrate, was collected by filtration and dissolved in a small amount of dichloromethane. The solution was charged into a silica gel column (2.5 cm \times 10 cm). Mononuclear $(\text{Bu}_4\text{N})_2[\text{ReBr}_6]$ was obtained from the second band by eluting with dichloromethane/acetonitrile = 10:1 (v/v) and characterized by elemental analysis and UV-vis absorption spectrum.

$(\text{Bu}_4\text{N})_2[\{\text{Re}_6\text{Se}_6\text{Br}_2\}\text{Br}_6]$ ($(\text{Bu}_4\text{N})_2[\mathbf{2a-Se}]$ and $(\text{Bu}_4\text{N})_2[\mathbf{2b-Se}]$). The first orange band eluted with dichloromethane/acetonitrile = 50:1 (v/v) was collected and evaporated to dryness. The residual orange solid was dissolved in acetonitrile/toluene, and allowed to stand for several days. The red crystals obtained were collected by filtration and then dried in air. Yield as the isomeric mixture of $(\text{Bu}_4\text{N})_2[\mathbf{2a-Se}]$ and $(\text{Bu}_4\text{N})_2[\mathbf{2b-Se}]$: 138 mg (14%). Anal. Calcd for $\text{C}_{32}\text{H}_{72}\text{N}_2\text{Br}_8\text{Re}_6\text{Se}_6$: C, 14.16; H, 2.67; N, 1.03%. Found: C, 14.39; H, 2.57; N, 1.09%. The atomic ratio of Br to Re and Se determined by the X-ray fluorescence spectrum was Br/Re/Se = 8:6:6. The crystals (138 mg) dissolved in a small amount of dichloromethane were charged into a silica gel column (2.5 cm \times 20 cm). The band spreading in the column was eluted with dichloromethane, and the eluent was collected with every about 15 mL, giving 20 fractions. Each solution was evaporated to dryness and then recrystallized from acetonitrile/toluene. The complex $(\text{Bu}_4\text{N})_2[\mathbf{2a-Se}]$ was obtained from the 1-9 fractions. Yield: 60 mg (6%). Anal. Calcd for $\text{C}_{32}\text{H}_{72}\text{N}_2\text{Br}_8\text{Re}_6\text{Se}_6 \cdot 0.2\text{C}_7\text{H}_8$: C, 14.68; H, 2.71; N, 1.03%. Found C, 14.61; H, 2.66; N, 0.99. UV-vis/nm ($\epsilon/\text{M}^{-1}\text{cm}^{-1}$ in CH_3CN): 406 (sh, 3600), 323 (sh, 11400), 292 (sh, 19000), 264 (sh, 26400).⁷⁷Se NMR (δ/ppm in CD_3CN): -143.7.

The complex $(\text{Bu}_4\text{N})_2[\mathbf{2b-Se}]$ was obtained from the 15-20 fractions. Yield: 31 mg (3%). Anal. Calcd for $\text{C}_{32}\text{H}_{72}\text{N}_2\text{Br}_8\text{Re}_6\text{Se}_6 \cdot 0.2\text{C}_7\text{H}_8$: C, 14.68; H, 2.71; N, 1.03%. Found C, 14.61; H, 2.69; N, 1.06. UV-vis/nm ($\epsilon/\text{M}^{-1}\text{cm}^{-1}$ in CH_3CN): 403 (sh, 3550), 347 (sh, 7100), 256 (31300).⁷⁷Se NMR (δ/ppm in CD_3CN): -169.1, -178.3.

$(\text{Bu}_4\text{N})_3[\{\text{Re}_6\text{Se}_7\text{Br}\}\text{Br}_6]$ ($(\text{Bu}_4\text{N})_3[\mathbf{1-Se}]$). The third orange band eluted with dichloromethane/acetonitrile = 8/1(v/v) was collected and evaporated to dryness. The residual orange solid was dissolved in acetone/toluene, and allowed to stand for several days. The red crystals obtained were collected by filtration and then dried in air. Yield of $(\text{Bu}_4\text{N})_3[\mathbf{1-Se}]$: 40 mg (8%). Anal. Calcd for $\text{C}_{48}\text{H}_{108}\text{N}_3\text{Br}_8\text{Re}_6\text{Se}_6$: C, 19.50; H, 3.68; N, 1.42%. Found: C, 19.61; H, 3.53; N, 1.45%. The atomic ratio of Br to Re and Se determined by the X-ray fluorescence spectrum was Br/Re/Se = 7:6:7. UV-vis/nm ($\epsilon/\text{M}^{-1}\text{cm}^{-1}$ in CH_3CN): 419 (sh, 2200), 262 (28400).⁷⁷Se NMR (δ/ppm in CD_3CN): -199.9, -259.4.

$(\text{Bu}_4\text{N})[\{\text{Re}_6\text{Se}_5\text{Br}_3\}\text{Br}_6]$ ($(\text{Bu}_4\text{N})[\mathbf{3-Se}]$). The reported high temperature reaction method was modified slightly to prepare the hexarhenium(III) cluster.⁴⁷ Elemental rhenium (200 mg, 1.08 mmol), selenium (71 mg, 0.89 mmol), cesium bromide (38 mg, 0.18 mmol), and bromine (37 μL , 0.72 mmol) were

charged into a silica ampule (i.d. 8 mm \times o.d. 10 mm \times 10 cm), the ampule was evacuated thoroughly, and sealed under vacuum. The reactants were mixed vigorously and heated to 850 °C for 4.5 h, kept at 850 °C for 67 h, and then cooled to room temperature during 3.5 h. The product was dissolved in water, and a large amount of the black residue was removed by filtration. An orange solid, precipitated upon an addition of tetra-*n*-butylammonium bromide (0.75 g, 2.3 mmol) to the filtrate, was collected by filtration and dissolved in a small amount of dichloromethane. The solution was charged into a silica gel column (2.5 cm \times 20 cm). The first band eluted with dichloromethane was dried. The residual orange solid was dissolved in dichloromethane/diethyl ether, and allowed to stand for several days. The red crystals obtained were collected by filtration, and then dried in air. Yield of (Bu₄N)[3-Se]: 25 mg (3%). Anal. Calcd for C₁₆H₃₆NBr₉Re₆Se₅: C, 7.77; H, 1.47; N, 0.57%. Found: C, 8.10; H, 1.41; N, 0.55%. The atomic ratio of Br to Re and Se determined by the X-ray fluorescence spectrum was Br/Re/Se = 9:6:5. UV-vis/nm (ϵ /M⁻¹ cm⁻¹ in CH₂Cl₂): 392 (4600), 300 (sh, 18500). ⁷⁷Se NMR (δ /ppm in DMSO-*d*₆): -23.8, -70.9, -73.2, -100.6, -145.2 -159.6, -191.7.

Separation of (Bu₄N)_{4-n}[{Re₆S_{8-n}Br_n}Br₆] (n = 1, 2). The high temperature reaction method reported by Slougui et al. was employed to synthesize the hexarhenium(III) clusters.⁶² Elemental rhenium (402 mg, 2.15 mmol), sulfur (69.5 mg, 2.17 mmol), potassium bromide (85.4 mg, 0.72 mmol), and bromine (55 μ L, 1.07 mmol) were charged into a silica ampule (i.d. 8 mm \times o.d. 10 mm \times 10 cm), the ampule was evacuated thoroughly and sealed under vacuum. The sample was mixed vigorously and heated to 850 °C for 4.5 h, continued heating at 850 °C for 67 h, and then cooled to room temperature during 3.5 h. The solid was dissolved in water and black residue was removed by filtration. An orange solid, precipitated upon addition of tetra-*n*-butylammonium bromide (519 mg, 1.61 mmol) to the filtrate, was collected by filtration and dissolved in a small amount of dichloromethane. The solution was charged into a silica gel column (2.5 \times 10 cm).

(Bu₄N)₂[{Re₆S₆Br₂}Br₆] ((Bu₄N)₂[2a-S] and (Bu₄N)₂[2b-S]). The first orange band eluted with dichloromethane was collected and evaporated to dryness. The residual orange solid was dissolved in acetonitrile/toluene, and allowed to stand for several days. The red crystals obtained were collected by filtration, and then dried in air. Yield of the isomeric mixture of (Bu₄N)₂[2a-S] and (Bu₄N)₂[2b-S]: 330 mg (38%). Anal. Calcd for C₃₂H₇₂N₂Br₈Re₆S₆·0.5CH₃CN: C, 16.15; H, 3.02; N, 1.43%. Found C, 16.24; H, 2.96; N, 1.36. The crystals (330 mg) were dissolved in a small amount of dichloromethane, and the solution was charged into a silica gel column (2.5 \times 20 cm). The spread orange band in the column was eluted with dichloromethane, and the eluent was collected with every about 15 mL, affording 21 fractions. Each solution was evaporated to dryness, and then recrystallized from acetonitrile/toluene. The complex (Bu₄N)₂[2a-S] was obtained from the 1–12 fractions. The solid obtained was collected by filtration and dried in air. Yield 181 mg (21%). Anal. Calcd for C₃₂H₇₂N₂Br₈Re₆S₆: C, 15.79; H, 2.98; N, 1.15%. Found C, 16.08; H, 2.93; N, 1.20. UV-vis/nm (ϵ /M⁻¹ cm⁻¹ in acetonitrile): 350 (sh, 5700), 311 (sh, 11500), 256 (30400), 228 (40000).

The complex (Bu₄N)₂[2b-S] was obtained from the 19–21 fractions. Yield 38 mg (4%). Anal. Calcd for C₃₂H₇₂N₂Br₈Re₆S₆: C, 15.79; H, 2.98; N, 1.15%. Found C, 16.05; H, 2.97; N, 1.08. UV-vis/nm (ϵ /M⁻¹ cm⁻¹ in CH₃CN): 387 (3300), 325 (sh, 7700), 250(30000).

(Bu₄N)₂[{Re₆S₆Br₂}Br₆] ((Bu₄N)₂[2c-S]). The second orange band eluted with dichloromethane was collected and evaporated to dryness. The residual orange solid was dissolved in acetonitrile/toluene, and allowed to stand for several days. The red crystals obtained were collected by filtration, and then dried in air. Yield of (Bu₄N)₂[2c-S]: 11 mg (1%). Anal. Calcd for

C₃₂H₇₂N₂Br₈Re₆S₆·0.5CH₃CN·0.5C₇H₈: C, 17.53; H, 3.12; N, 1.40%; Found: C, 17.57; H, 3.12; N, 1.47%. UV-vis/nm (ϵ /M⁻¹ cm⁻¹ in acetonitrile); 384 (3500), 325 (sh, 8200), 249 (32700), 229 (39400).

(Bu₄N)₃[{Re₆S₇Br}Br₆] ((Bu₄N)₃[1-S]). The third orange band eluted with dichloromethane/acetonitrile = 20/1 (v/v) was collected and evaporated to dryness. The residual orange solid was dissolved in acetone/toluene, and allowed to stand for several days. The red crystals obtained were collected by filtration and then dried in air. Yield of (Bu₄N)₃[1-S]: 145 mg (16%). C₄₈H₁₀₈N₃Br₇Re₆S₇: C, 21.93; H, 4.14; N, 1.60%; Found: C, 21.96; H, 4.03; N, 1.65%. UV-vis/nm (ϵ /M⁻¹ cm⁻¹ in acetonitrile); 313 (sh, 8600), 277 (sh, 23600).

Physical Measurements. UV-vis absorption spectra were recorded on a JASCO U-550 spectrophotometer. ⁷⁷Se NMR spectra were recorded on a 95.39 MHz JEOL ECA-500 spectrometer. All peaks were referred to the signal of (CH₃)₂Se in C₆D₆ as δ = 0. For photophysical measurements, sample solids were placed between two nonfluorescent glass plates, and the solution samples were deoxygenated by purging an Ar gas stream at least 15 min, and then sealed. For spectroscopic and photophysical experiments at 80 or 95 K, a temperature (\pm 0.1 K) was controlled by using a liquid-N₂ cryostat system (Oxford Instruments). A pulsed Nd³⁺:YAG laser (Lotis TII LS-2137, 355 nm, fwhm 18 ns) was used as an exciting light source for the measurements of the emission spectrum in the wavelength region (λ) of 550–1000 nm and the emission lifetime. Corrected emission spectra were recorded on a Hamamatsu Photonics PMA-12 in the 550 < λ < 1000 nm. In 1000 < λ < 1500 nm, the corrected emission spectra were measured on a Horiba Fluorolog-3 with a liquid N₂-cooled InGaAs detector with the excitation wavelength at 355 nm. The emission lifetime was determined by using a streak camera (Hamamatsu Photonics, C4334).

Results

Separation of the Complexes. The {Re₆Se₆Br₂}⁴⁺ and {Re₆Se₇Br}Br₆³⁺ complexes, [{Re₆Se₆Br₂}Br₆]²⁻ and [{Re₆Se₇Br}Br₆]³⁻, were prepared by the literature methods reported by Yarovoi et al.⁷⁷ The mixture of the {Re₆Se₆Br₂}⁴⁺ and {Re₆Se₇Br}Br₆³⁺ complexes including their geometrical isomers was separated by silica gel column chromatography. The {Re₆Se₆Br₂}⁴⁺ and {Re₆Se₇Br}Br₆³⁺ complexes were obtained from the first and third eluted bands, respectively. The isomers of the {Re₆Se₆Br₂}⁴⁺ complex were isolated by successive column chromatography through collecting 20 dichloromethane fractions. On the basis of the UV-vis absorption band shape and ⁷⁷Se NMR spectrum, the complex obtained from the 1–9 fractions was assigned to [2a-Se]²⁻ and that obtained from the 15–20 fractions was [2b-Se]²⁻. The ⁷⁷Se NMR spectra of the 10–14 fractions indicated that the fractions were the mixture of the isomers. As shown in Figure 2, the UV-vis absorption spectral band shape of [2a-Se]²⁻ in acetonitrile was different from that of [2b-Se]²⁻. The ⁷⁷Se NMR spectra of [2a-Se]²⁻ and [2b-Se]²⁻ in CD₃CN are shown in Figure 3. The ⁷⁷Se NMR spectrum of [2a-Se]²⁻ showed a signal at -143.7 ppm, while [2b-Se]²⁻ exhibited two signals at -169.1 and -178.3 ppm with the approximate integrated intensity ratio of 1:2. Figure 1 summarizes the possible isomers of the {Re₆Q₆Br₂}⁴⁺ complexes. The {Re₆Q₆Br₂}⁴⁺ complex has potentially three isomers, which are D_{3d} and two C_{2v} symmetric structures. The six capping selenide atoms in the D_{3d} isomer sit essentially in the same coordination environments, indicating that the ⁷⁷Se NMR spectrum should

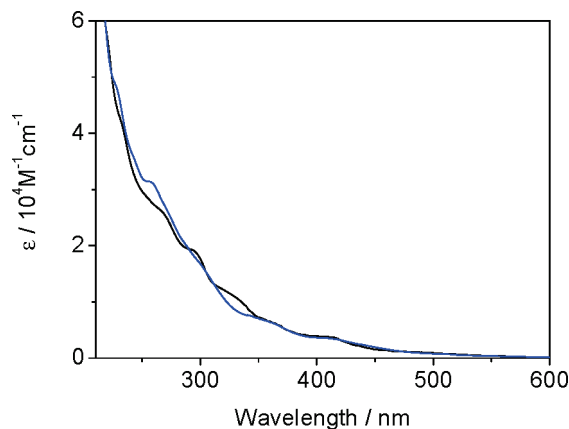


Figure 2. UV-vis absorption spectra of the D_{3d} isomer ($[2\mathbf{a}\text{-Se}]^{2-}$, black) and C_{2v} isomer ($[2\mathbf{b}\text{-Se}]^{2-}$, blue) for $(\text{Bu}_4\text{N})_2[\{\text{Re}_6\text{Se}_6\text{Br}_2\}\text{Br}_6]$ in acetonitrile at room temperature.

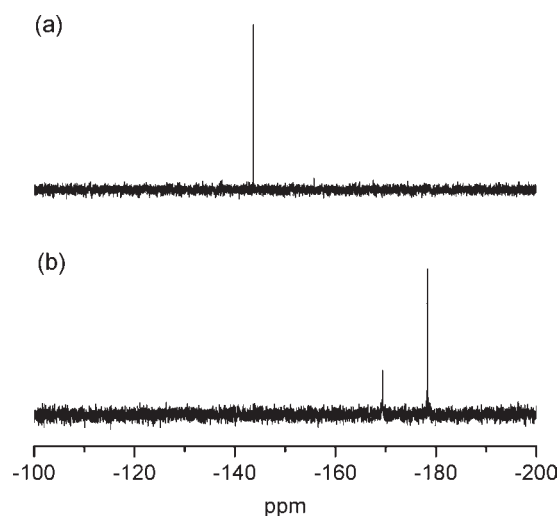


Figure 3. ^{77}Se NMR spectra for the D_{3d} isomer (a) and C_{2v} isomer (b) of $(\text{Bu}_4\text{N})_2[\{\text{Re}_6\text{Se}_6\text{Br}_2\}\text{Br}_6]$ in CD_3CN at room temperature.

show one signal. On the other hand, one of the two C_{2v} isomers should exhibit two signals with the integral intensity ratio of 1:2 (C_{2v} (a)) or three signals with the ratio of 1:1:1 (C_{2v} (b)). Therefore, $[2\mathbf{a}\text{-Se}]^{2-}$ is assignable to the D_{3d} isomer and $[2\mathbf{b}\text{-Se}]^{2-}$ is the C_{2v} isomer(s). At the present stage of the investigation, it is unclear whether $[2\mathbf{b}\text{-Se}]^{2-}$ is a pure product of either C_{2v} isomer or mixture.

The $\{\text{Re}_6\text{Se}_5\text{Br}_3\}^{5+}$ complex, $[\{\text{Re}_6\text{Se}_5\text{Br}_3\}\text{Br}_6]^-$ ($[3\text{-Se}]^-$), was prepared by the method reported by Perrin et al.⁴⁷ The complex was isolated and purified by silica gel column chromatography. The ^{77}Se NMR spectrum of $[3\text{-Se}]^-$ in CD_3CN showed seven signals (Supporting Information, Figure S1). The C_{3v} isomer should show three signals with the integrated intensity ratio of 1:1:3, while the C_s isomers exhibit three signals with the ratio of 1:2:2 (C_s (a)) or four signals with the ratio of 1:1:1:2 (C_s (b)). Therefore, $[3\text{-Se}]^-$ showing seven signals in the ^{77}Se NMR spectrum will be the mixture of the isomers.

The thiobromide-capped complexes including their geometrical isomers were prepared by the literature method reported by Slougui et al.⁶² The mixture of the $\{\text{Re}_6\text{S}_7\text{Br}\}^{3+}$ and $\{\text{Re}_6\text{S}_6\text{Br}_2\}^{4+}$ complexes was sepa-

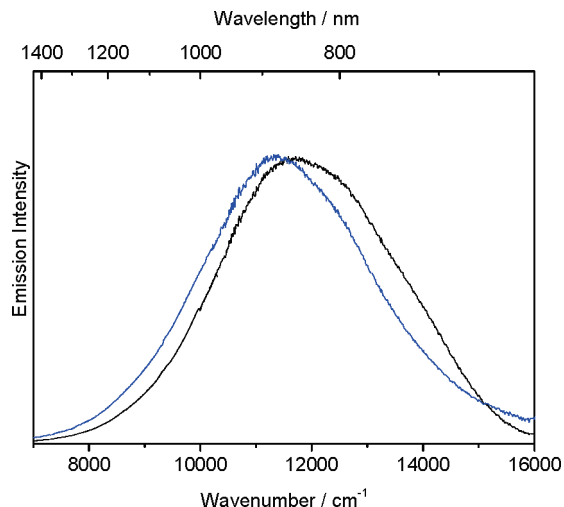


Figure 4. Emission spectra for the D_{3d} isomer ($(\text{Bu}_4\text{N})_2[2\mathbf{a}\text{-Se}]$ (black)) and C_{2v} isomer ($(\text{Bu}_4\text{N})_2[2\mathbf{b}\text{-Se}]$ (blue)) of $(\text{Bu}_4\text{N})_2[\{\text{Re}_6\text{Se}_6\text{Br}_2\}\text{Br}_6]$ in the crystalline phase at 296 K.

rated by the analogous procedures with those of the selenobromide complexes. The first eluted band in column chromatography was the mixture of $[2\mathbf{a}\text{-S}]^{2-}$ and $[2\mathbf{b}\text{-S}]^{2-}$, while the second eluted band was assigned to $[2\mathbf{c}\text{-S}]^{2-}$. The $\{\text{Re}_6\text{S}_7\text{Br}\}^{3+}$ complex was obtained from the third band. The first eluted band was evaporated to dryness, and the residue dissolved in dichloromethane was charged into a silica gel column. The eluted solution was fractionally collected, and then the complexes isolated were assigned to the two isomers $[2\mathbf{a}\text{-S}]^{2-}$ and $[2\mathbf{b}\text{-S}]^{2-}$ on the basis of the UV-vis absorption spectroscopy. Figure S2 (Supporting Information) shows the UV-vis absorption spectra of the three $\{\text{Re}_6\text{S}_6\text{Br}_2\}^{4+}$ complexes in acetonitrile. The absorption spectral band shapes of the isomer $[2\mathbf{b}\text{-S}]^{2-}$ and $[2\mathbf{c}\text{-S}]^{2-}$ were very similar each other, while that of $[2\mathbf{a}\text{-S}]^{2-}$ was somewhat different from those of $[2\mathbf{b}\text{-S}]^{2-}$ and $[2\mathbf{c}\text{-S}]^{2-}$. Almost half of the total yield of $\{\text{Re}_6\text{S}_6\text{Br}_2\}^{4+}$ complex was $[2\mathbf{a}\text{-S}]^{2-}$, and $[2\mathbf{b}\text{-S}]^{2-}$ and $[2\mathbf{c}\text{-S}]^{2-}$ were minor products. It was assigned that $[2\mathbf{a}\text{-S}]^{2-}$ was the D_{3d} symmetric isomer and $[2\mathbf{b}\text{-S}]^{2-}$ and $[2\mathbf{c}\text{-S}]^{2-}$ were the C_{2v} isomers, as described in the following section.

Spectroscopic and Photophysical Properties. All of the complexes studied in the present work showed luminescence at room temperature in both crystalline and solution phases. The emission spectra of the two isomers $[2\mathbf{a}\text{-Se}]^{2-}$ and $[2\mathbf{b}\text{-Se}]^{2-}$ in the crystalline phase and in acetonitrile at 296 K are shown in Figures 4 and 5. The emission spectra of the other chalcobromide-capped complexes in the crystalline phase and in acetonitrile at 296 K are shown in Supporting Information, Figures S3–S8. Table 1 summarizes the emission maxima (λ_{em}), lifetimes (τ_{em}), and quantum yields (Φ_{em}) of the chalcobromide-capped complexes, together with those of the related chalcogenide-capped complexes. The broad emission spectral shapes of the chalcobromide-capped complexes resemble those of the $\{\text{Re}_6\text{Q}_8\}^{2+}$ ($\text{Q} = \text{S}, \text{Se}$) complexes. The λ_{em} values are observed in the wavelength region of 868–968 nm in acetonitrile and 853–915 nm in the crystalline phase at 296 K. The λ_{em} values of the chalcobromide-capped complexes were observed beyond visible region. Therefore, the emission from these complexes

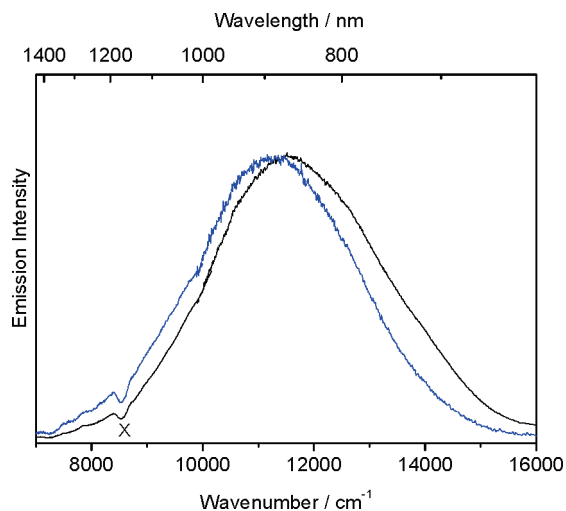


Figure 5. Emission spectra for the D_{3d} isomer ($(\text{Bu}_4\text{N})_2[\mathbf{2a}\text{-Se}]$) (black) and C_{2v} isomer ($(\text{Bu}_4\text{N})_2[\mathbf{2b}\text{-Se}]$) (blue) of $(\text{Bu}_4\text{N})_2[\text{Re}_6\text{Se}_6\text{Br}_2]\text{Br}_6$ in acetonitrile at 296 K. The feature with \times is due to instrumental artifact.

could not be confirmed by naked eyes. The emission lifetimes of the complexes in acetonitrile at 296 K with 0.1–2.6 μs indicate that the emissive excited-state of the chalcobromide-capped hexarhenium(III) complex possesses the spin-triplet excited-state. The λ_{em} value observed for the $\{\text{Re}_6\text{Q}_7\text{Br}\}^{3+}$ or $\{\text{Re}_6\text{Q}_6\text{Br}_2\}^{4+}$ complex in acetonitrile at 296 K was almost the same with or shifted to the longer wavelength, respectively, as compared with that of the relevant complex in the crystalline phase. The spectral shift was small for the $\{\text{Re}_6\text{Q}_7\text{Br}\}^{3+}$ or $\{\text{Re}_6\text{Q}_6\text{Br}_2\}^{4+}$ complex (–1 to +23 nm) as compared with that of the $\{\text{Re}_6\text{Se}_5\text{Br}_3\}^{5+}$ complex, which showed a longer wavelength emission spectral shift by +53 nm on going from the crystalline phase to an acetonitrile solution.

The $\{\text{Re}_6\text{Se}_6\text{Br}_2\}^{4+}$ complexes were separated as two isomers: the D_{3d} isomer [$\mathbf{2a}\text{-Se}$] $^{2-}$ and C_{2v} isomer(s) [$\mathbf{2b}\text{-Se}$] $^{2-}$ as described before. The D_{3d} isomer showed a single exponential emission decay ($\tau_{\text{em}} = 2.60 \mu\text{s}$) at around $\lambda_{\text{em}} = 868 \text{ nm}$ ($\Phi_{\text{em}} = 0.014$) in acetonitrile at 296 K. The C_{2v} isomer(s) showed longer wavelength emission ($\lambda_{\text{em}} = 885 \text{ nm}$) with the lower emission quantum yield ($\Phi_{\text{em}} = 0.0039$) and shorter emission lifetime ($\tau_{\text{em}} = 0.785 \mu\text{s}$) as compared with the relevant value of the D_{3d} isomer. Such results have been also observed for the $\{\text{Re}_6\text{S}_6\text{Br}_2\}^{4+}$ analogues. The λ_{em} values of the $\{\text{Re}_6\text{S}_6\text{Br}_2\}^{4+}$ isomers are 889–919 nm in the crystalline phase and in acetonitrile. The τ_{em} and Φ_{em} values of the C_{2v} isomers, [$\mathbf{2b}\text{-S}$] $^{2-}$ and [$\mathbf{2c}\text{-S}$] $^{2-}$, are significantly shorter and lower, respectively, than the relevant value of the D_{3d} isomer, [$\mathbf{2a}\text{-S}$] $^{2-}$ (the assignment of the isomer is described in the following section).

The emission spectra of the $\{\text{Re}_6\text{Se}_6\text{Br}_2\}^{4+}$ complexes including their geometrical isomers in the crystalline phases at 80 K are shown in Figures 6. The emission spectra of the other chalcobromide-capped complexes in the crystalline phase at 80 K are shown in Supporting Information, Figures S9–S11. Upon cooling from 298 to 80 K in the crystalline phase, the λ_{em} values of the chalcobromide-capped complexes were shifted to the longer wavelength by +42 to +57 nm. The temperature (T)-dependence of the emission spectrum of $[\{\text{Re}_6\text{S}_8\}\text{X}_6]^{4-}$

($\text{X} = \text{Cl}, \text{Br}, \text{I}$) has been reported by our research group and Gray et al.^{8,11} The T -dependences of the emission properties of the hexamolybdenum(II) complex $[\{\text{Mo}_6\text{Cl}_8\}\text{Cl}_6]^{2-}$ that is isoelectronic and isostructural to the hexarhenium(III) complexes have been also reported.^{23,27} The longer wavelength shift of the emission from the chalcobromide-capped complexes upon cooling from 298 to 80 K is similar to that of the chalcogenide-capped hexarhenium(III) or halide-capped hexamolybdenum(II) complexes.

The emission from the chalcobromide-capped complexes in the crystalline phases showed multiexponential decays at both 296 and 80 K. In the solid state, excitation energy migration proceeds sometimes very efficiently, and the excitation energy is trapped at various crystal defect sites. Therefore, we suppose that non-single exponential emission decays observed for these complexes in the crystalline phase would be due to the presence of the crystal defects.

Discussion

Characterization of the Isomers of $[\{\text{Re}_6\text{Q}_6\text{Br}_2\}\text{Br}_6]^{2-}$ ($\text{Q} = \text{Se}, \text{S}$). In our chromatographic separation of the $\{\text{Re}_6\text{Se}_6\text{Br}_2\}^{4+}$ isomers, the D_{3d} isomer eluted first, and the C_{2v} isomer(s) followed. Each D_{3d} and C_{2v} isomer was isolated and the structure of the isomer was confirmed by the ^{77}Se NMR spectroscopy. Yarovoi et al. reported the abundance of the D_{3d} and two C_{2v} isomers in the mixture of $[\{\text{Re}_6\text{Se}_6\text{Br}_2\}\text{Br}_6]^{2-}$ to be $D_{3d}:C_{2v}:C_{2v} = 61:27:12$ as estimated by the ^{77}Se NMR technique.⁷⁷ Shestopalov et al. calculated the bonding energies of the $[\{\text{Re}_6\text{Q}_6\text{Br}_2\}\text{Br}_6]^{2-}$ ($\text{Q} = \text{S}, \text{Se}$) isomers and demonstrated that the most stable isomer was the D_{3d} symmetric structure.⁸⁶ They also reported that the reaction of the isomeric mixture of $[\{\text{Re}_6\text{S}_6\text{Br}_2\}\text{Br}_6]^{2-}$ with molten PPh_3 gave *trans*- $[\{\text{Re}_6\text{S}_6\text{Br}_2\}\text{Br}_4(\text{PPh}_3)_2]$ from the D_{3d} isomer of $[\{\text{Re}_6\text{S}_6\text{Br}_2\}\text{Br}_6]^{2-}$ and *cis*- $[\{\text{Re}_6\text{S}_6\text{Br}_2\}\text{Br}_4(\text{PPh}_3)_2]$ from the C_{2v} isomer, and they proposed that the isomer ratio of $[\{\text{Re}_6\text{S}_6\text{Br}_2\}\text{Br}_6]^{2-}$ was similar to those of the selenide analogues and the original isomer ratio remained in the terminal ligand substitution of the bromides by PPh_3 .⁸⁶ Fontaine et al. reported single crystals of the mixture of $[\{\text{Re}_6\text{S}_6\text{Br}_2\}\text{Br}_6]^{2-}$ ($C_{2v}(\text{a})$) and $[\{\text{Re}_6\text{S}_5\text{Br}_3\}\text{Br}_6]^{-}$ ($C_s(\text{a})$) isomers.⁸⁹ Furthermore, their density functional theory (DFT) calculations on $[\{\text{Re}_6\text{S}_6\text{Br}_2\}\text{Br}_6]^{2-}$ demonstrated that the energy differences between these isomers were rather small, and the $C_{2v}(\text{b})$ isomer of $[\{\text{Re}_6\text{S}_6\text{Br}_2\}\text{Br}_6]^{2-}$ was slightly unstable as compared with other isomers.⁸⁹ The DFT calculations of $[\{\text{Re}_6\text{S}_{8-n}\text{Cl}_n\}\text{Cl}_6]^{n-4}$ by Deluzet et al. showed that the D_{3d} isomer was the most stable in energy among three $[\{\text{Re}_6\text{S}_6\text{Cl}_2\}\text{Cl}_6]^{2-}$ isomers.⁹⁷ In the present study, the D_{3d} isomer was approximately half of the total yield among the $\{\text{Re}_6\text{Se}_6\text{Br}_2\}^{4+}$ isomers. The result is consistent with the estimation of the ratio of the three geometrical isomers using the ^{77}Se NMR study in the mixture of the $\{\text{Re}_6\text{Se}_6\text{Br}_2\}^{4+}$ isomers.⁷⁷

It is worth noting that the emission spectroscopic and photophysical data are sensitive to the geometrical structures of the isomers and, thus, are powerful to distinguish

(97) Deluzet, A.; Duclausaud, H.; Sautet, P.; Borshch, S. A. *Inorg. Chem.* **2002**, *41*, 2537–2542.

Table 1. Photophysical Data of the Hexarhenium(III) Complexes in Acetonitrile at 296 K and in the Crystalline Phase at 296 and 80 K

complex	296 K in acetonitrile					296 K in the crystalline phase	80 K in the crystalline phase
	λ_{em}/nm	Φ_{em}	$\tau_{em}/\mu s$	$k_r/10^3 s^{-1}$	$k_{nr}/10^4 s^{-1}$	λ_{em}/nm	λ_{em}/nm
$\{[Re_6Se_8](CN)_6\}^{4-}$	720 ^{a,b}	0.140 ^{a,b}	17.1 ^{a,b}	8.2	5.0		
$\{[Re_6Se_8](NCS)_6\}^{4-}$	730 ^{a,c}	0.15 ^{a,c}	11.8 ^{a,c}	12.7	7.2		
$\{[Re_6Se_7Br]Br_6\}^{3-}$ ($[1-Se]^{3-}$)	910	0.016	1.87	8.6	53	886	938
$\{[Re_6Se_6Br_2]Br_6\}^{2-}$ D_{3d} isomer ($[2a-Se]^{2-}$)	868	0.014	2.60	5.4	38	853	900
$\{[Re_6Se_6Br_2]Br_6\}^{2-}$ C_{2v} isomer ($[2b-Se]^{2-}$)	885	0.0039	0.785	5.0	130	880	923
$\{[Re_6Se_5Br_3]Br_6\}^{2-}$ ($[3-Se]^{-}$)	968	0.00034	0.768	0.44	440	915	930 ^d
$\{[Re_6S_8]Cl_6\}^{4-}$	770 ^{a,e}	0.039 ^{a,e}	6.3 ^{a,e}	6.2	15.3	770 ^f	858 ^f
$\{[Re_6S_8]Br_6\}^{4-}$	780 ^{a,e}	0.018 ^{a,e}	5.4 ^{a,e}	3.3	18.2	780 ^f	884 ^f
$\{[Re_6S_8]I_6\}^{4-}$	800 ^{a,e}	0.015 ^{a,e}	4.4 ^{a,e}	3.4	22.4	800 ^f	895 ^f
$\{[Re_6S_8](CN)_6\}^{4-}$	720 ^{a,b}	0.056 ^{a,b}	11.2 ^{a,b}	5.0	8.4	720 ^f	820 ^f
$\{[Re_6S_8](NCS)_6\}^{4-}$	745 ^{a,c}	0.091 ^{a,c}	10.4 ^{a,c}	8.8	8.7	745 ^f	847 ^f
$\{[Re_6S_7Br]Br_6\}^{3-}$ ($[1-S]^{3-}$)	885	0.0021	0.450	4.7	220	886	928
$\{[Re_6S_6Br_2]Br_6\}^{2-}$ D_{3d} isomer ($[2a-S]^{2-}$)	895	0.00065	0.295	2.2	340	889	946
$\{[Re_6S_6Br_2]Br_6\}^{2-}$ C_{2v} isomer ($[2b-S]^{2-}$)	917	0.00023	0.108	2.1	930	898	953
$\{[Re_6S_6Br_2]Br_6\}^{2-}$ C_{2v} isomer ($[2c-S]^{2-}$)	919	0.00025	0.121	2.1	830	896	947

^aAt 298 K. ^bRef 4. ^cRef 9. ^dAt 95 K. ^eRef 3. ^fRef 100.

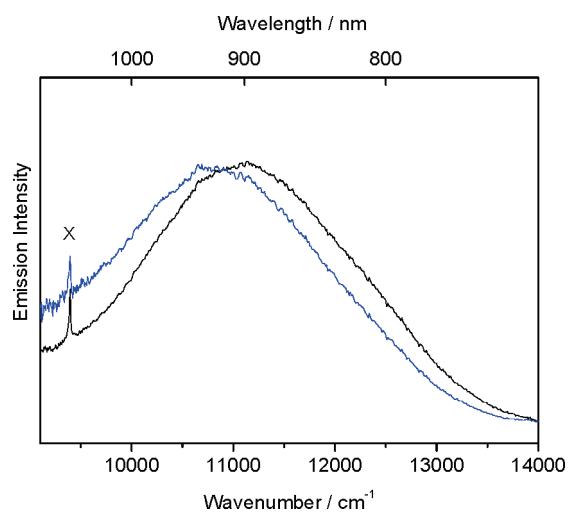


Figure 6. Emission spectra for the D_{3d} isomer ($(Bu_4N)_2[2a-Se]$) (black) and the C_{2v} isomer ($(Bu_4N)_2[2b-Se]$) (blue) of $(Bu_4N)_2[Re_6Se_6Br_2]Br_6$ in the crystalline phase at 80 K. The feature with \times is due to instrumental artifact.

the isomers. In practice, the D_{3d} isomer showed larger Φ_{em} , longer τ_{em} , and shorter λ_{em} values than the relevant value of the corresponding C_{2v} isomer(s). The discussion on characterization of the $\{Re_6S_6Br_2\}^{4+}$ isomers can be made on the basis of the photophysical properties of the complexes of the eluted solutions in column chromatography and the yields of the complexes. The D_{3d} isomer eluted first in silica gel column chromatography was the major product and showed emission in the shorter wavelength with a larger Φ_{em} and a longer τ_{em} in acetonitrile at 296 K as compared with the relevant value of the C_{2v} isomers eluted as the second band. The observations analogous to those of the $\{Re_6S_6Br_2\}^{4+}$ isomers have been also confirmed for the $\{Re_6Se_6Br_2\}^{4+}$ complexes. On the basis of these experimental results, $[2a-S]^{2-}$ can be assignable to the D_{3d} isomer and the other two complexes ($[2b-S]^{2-}$ and $[2c-S]^{2-}$) are the C_{2v} isomers. It should be noted that $(Bu_4N)_2[2b-S]$ and $(Bu_4N)_2[2c-S]$ shows almost analogous UV-vis absorption/emission spectral band shapes and photophysical data, although $(Bu_4N)_2[2b-S]$ and $(Bu_4N)_2[2c-S]$ were obtained separately by column

chromatography. Therefore, $(Bu_4N)_2[2b-S]$ and $(Bu_4N)_2[2c-S]$ might be identical with each other.

Photoluminescent Properties of Chalcobromide-capped Hexarhenium Complexes. For a series of the chalcobromide-capped complexes with terminal bromide ligands having the $\{Re_6Q_7Br\}^{3+}$, $\{Re_6Q_6Br_2\}^{4+}$, or $\{Re_6Se_5Br_3\}^{5+}$ core, all of the complex showed broad emission spectra with the emission lifetime of 0.1–2.6 μs . Furthermore, the emission spectral band shape and maximum wavelength of the $\{Re_6Q_7Br\}^{3+}$ and $\{Re_6Q_6Br_2\}^{4+}$ complexes in the crystalline state were similar to those in acetonitrile. These spectral and photophysical properties of the complexes including a longer wavelength shift of the λ_{em} value upon cooling from 296 to 80 K are very analogous to those observed for the $\{Re_6Q_8\}^{2+}$ complexes. Therefore, the emission spectral and photophysical properties of the chalcobromide-capped complexes can be explained along the similar context with those of $\{Re_6Q_8\}^{2+}$ and the excited-states of the chalcobromide-capped hexarhenium(III) complexes are best characterized by the hexarhenium core-centered excited-states. In the case of the $\{Re_6Se_5Br_3\}^{5+}$ complex, however, the λ_{em} value in acetonitrile (968 nm) was shifted to the longer wavelength as compared with that in the crystalline phase (915 nm). Such spectroscopic behaviors are very similar to those of the $\{Re_6S_8\}^{2+}$ complexes bearing redox active N-heteroaromatic terminal ligands (L: 4,4'-bipyridine or pyrazine) and, recently, we have reported that the phenomena will be explained by the contribution of the metal (Re)-to-ligand (L) charge transfer (MLCT) character to the $\{Re_6S_8\}^{2+}$ core-centered excited-state.⁹⁸ It is therefore that the charge transfer character might contribute to the excited-state of the $\{Re_6Se_5Br_3\}^{5+}$ complex with the hexarhenium core-centered character. It is worth noting, furthermore, that Φ_{em} and τ_{em} become smaller and shorter, respectively, in the order of $\{[Re_6S_8]Br_6\}^{4-}$ ($\Phi_{em} = 0.018$ and $\tau_{em} = 5.4 \mu s$) > $\{[Re_6S_7Br]Br_6\}^{3-}$ ($\Phi_{em} = 0.0021$ and $\tau_{em} = 0.45 \mu s$) > the D_{3d} isomer of $\{[Re_6S_6Br_2]Br_6\}^{2-}$ ($\Phi_{em} = 0.00065$ and $\tau_{em} = 0.295 \mu s$) > the C_{2v} isomers of $\{[Re_6S_6Br_2]Br_6\}^{2-}$ ($\Phi_{em} = 0.00023$ – 0.00025 and $\tau_{em} = 0.108$ – $0.121 \mu s$). Although

(98) Yoshimura, T.; Suo, C.; Tsuge, K.; Ishizaka, S.; Nozaki, K.; Sasaki, Y.; Kitamura, N.; Shinohara, A. *Inorg. Chem.* **2010**, *49*, 531–540.

the photophysical data of $[\{\text{Re}_6\text{Se}_8\}\text{Br}_6]^{4-}$ have not been obtained, the decreasing order of the Φ_{em} and τ_{em} values are in the sequence of $[\{\text{Re}_6\text{Se}_7\text{Br}\}\text{Br}_6]^{3-}$ ($\Phi_{\text{em}} = 0.016$ and $\tau_{\text{em}} = 1.87 \mu\text{s}$) \approx the D_{3d} isomer of $[\{\text{Re}_6\text{Se}_6\text{Br}_2\}\text{Br}_6]^{2-}$ ($\Phi_{\text{em}} = 0.014$ and $\tau_{\text{em}} = 2.60 \mu\text{s}$) $>$ the C_{2v} isomer of $[\{\text{Re}_6\text{Se}_6\text{Br}_2\}\text{Br}_6]^{2-}$ ($\Phi_{\text{em}} = 0.0039$ and $\tau_{\text{em}} = 0.785 \mu\text{s}$) $>$ $[\{\text{Re}_6\text{Se}_5\text{Br}_3\}\text{Br}_6]^{-}$ ($\Phi_{\text{em}} = 0.00034$ and $\tau_{\text{em}} = 0.768 \mu\text{s}$). The tendency is similar for both thiobromide- and selenobromide-capped complexes. Apparently, the photoluminescence becomes weaker as the increase in the number of the capping bromide ligand in the $\{\text{Re}_6\text{Q}_{8-n}\text{Br}_n\}^{n+2}$ core. Furthermore, the higher symmetric structure of the $\{\text{Re}_6\text{Q}_{8-n}\text{Br}_n\}^{n+2}$ core in the ground-state ($n = 0-2$) showed more intense luminescence. Gray et al. reported that the O_h symmetric structure of the $\{\text{Re}_6\text{S}_8\}^{2+}$ core in the ground-state is distorted to D_{4h} symmetry in the emissive excited-state.¹⁰ The structural distortion between the ground- and excited-states would be thus one of the factors governing the spectroscopic and photophysical properties of the hexarhenium(III) complexes.

To discuss further the excited-state characteristics of the complexes, the radiative (k_r) and nonradiative decay rate constants (k_{nr}) in acetonitrile were calculated based on the relations of $k_r = \Phi_{\text{em}}/\tau_{\text{em}}$, and $\Phi_{\text{em}} = k_r/(k_r + k_{nr})$. Table 1 also includes the k_r and k_{nr} values together with the λ_{em} , Φ_{em} , and τ_{em} values. The k_r values of the chalcogenide- and chalcobromide-capped $\{\text{Re}_6\text{Q}_{8-n}\text{Br}_n\}^{n+2}$ ($n = 0, 1, 2$) complexes in acetonitrile at 296 K fall in the range $2.1 \times 10^3-1.3 \times 10^4 \text{ s}^{-1}$. The small difference in the k_r value of the complex having the $\{\text{Re}_6\text{Q}_{8-n}\text{Br}_n\}^{n+2}$ core would indicate that the emissive excited-state is localized largely on the hexarhenium(III) core similar to that of the $\{\text{Re}_6\text{Q}_8\}^{2+}$ complexes. The Φ_{em} and τ_{em} values of the selenide complexes in acetonitrile are larger and longer, respectively, than the relevant value of the sulfide analogues. In contrast to k_r , the k_{nr} values of a series of the $\{\text{Re}_6\text{Q}_{8-n}\text{Br}_n\}^{n+2}$ ($n = 0, 1, 2$) complexes vary significantly in the range of $5.0 \times 10^4-9.3 \times 10^6 \text{ s}^{-1}$, demonstrating that the Φ_{em} and τ_{em} values are governed by the nonradiative decay rate constant. The results in Table 1 also indicate that the k_{nr} value is dependent on the number of the capping bromide ligand and the symmetry of the $\{\text{Re}_6\text{Q}_{8-n}\text{Br}_n\}^{n+2}$ core. The k_{nr} values of the sulfide-capped complexes $\{\text{Re}_6\text{S}_8\}^{2+}$ are 1.5 times larger than those of the selenide analogues, while those of the $\{\text{Re}_6\text{S}_7\text{Br}\}^{3+}$ and $\{\text{Re}_6\text{S}_6\text{Br}_2\}^{4+}$ are about 4 and 7–9 times larger, respectively, as compared with the relevant value of the selenide analogues. It is known that the emission lifetimes of the hexarhenium(III) complexes in solution are dependent on the nature of the terminal ligand, and such results have been often discussed on the basis of the energy gap dependence of k_{nr} .^{1,4,8,9} In practice, a linear correlation between E^{em} ($1/\lambda_{\text{em}}$) and $\ln k_{nr}$ for a series of $[\{\text{Re}_6\text{S}_8\}\text{X}_6]^{4-}$ ($\text{X} = \text{Cl}, \text{Br}, \text{I}, \text{CN}, \text{or NCS}$) in acetonitrile at 298 K was previously reported.^{4,9} Gray et al. also reported a linear correlation between $\ln k_{nr}$ and E^{em} for both $\{\text{Re}_6\text{S}_8\}^{2+}$ and $\{\text{Re}_6\text{Se}_8\}^{2+}$ with terminal halide, cyanide, solvent molecules, or mixed phosphine-halide in dichloromethane at 296 K.^{1,8} To obtain further information about nonradiative decay of the complexes, therefore, the k_{nr} data were analyzed on the basis of the energy gap law. The energy gap dependence of

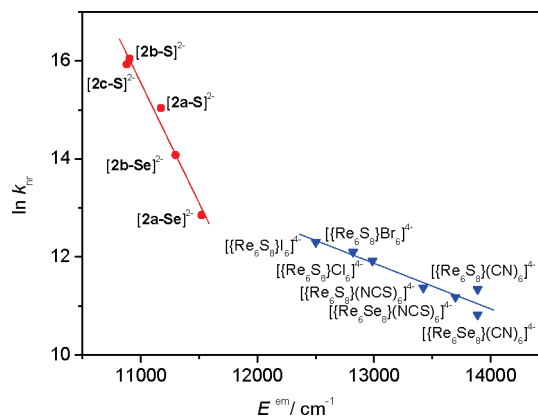


Figure 7. Correlation between $\ln k_{nr}$ and emission maximum (E^{em} (cm^{-1})) for $[\{\text{Re}_6\text{Q}_6\text{Br}_2\}\text{Br}_6]^{2-}$ ($\text{Q} = \text{S}, \text{Se}$) and $[\text{Re}_6\text{Q}_8\text{X}_6]^{4-}$ ($\text{Q} = \text{S}, \text{X} = \text{Cl}, \text{Br}, \text{I}, \text{CN}, \text{NCS}$; $\text{Q} = \text{Se}, \text{X} = \text{NCS}, \text{CN}$).

$\ln k_{nr}$ is given by eq 1.⁹⁹

$$\ln k_{nr} \propto \ln \beta - \frac{\gamma E^{\text{em}}}{h\omega} \quad (1)$$

where β represents the nuclear momentum matrix element which couples the excited vibrational states with the ground vibrational states, $E^{\text{em}} = 1/\lambda_{\text{em}}$, h is the Planck's constant, ω is the angular frequency of the vibration(s) responsible for nonradiative decay, and γ is given by

$$\gamma = \ln \left(\frac{E^{\text{em}}}{h\omega S} \right) - 1 \quad (2)$$

where S is the parameter related to the vibrational displacement between the ground- and excited-states. Although E^{em} is included in γ , this contribution to an energy gap plot has been reported to be minor.⁹⁹ Therefore, $\ln k_{nr}$ should correlate linearly with E^{em} under the assumptions of the energy gap law. Figure 7 shows an energy gap dependence of $\ln k_{nr}$ for $[\{\text{Re}_6\text{Q}_6\text{Br}_2\}\text{Br}_6]^{2-}$ in acetonitrile at 296 K, together with that of a $[\{\text{Re}_6\text{Q}_8\}\text{X}_6]^{4-}$ ($\text{Q} = \text{S}, \text{X} = \text{Cl}, \text{Br}, \text{I}, \text{CN}, \text{or NCS}$; $\text{Q} = \text{Se}, \text{X} = \text{CN or NCS}$) series in acetonitrile. It is very clear that the data for $[\{\text{Re}_6\text{Q}_6\text{Br}_2\}\text{Br}_6]^{2-}$ fall on a straight line, demonstrating that the nonradiative decay process is very similar for the $\{\text{Re}_6\text{Q}_6\text{Br}_2\}^{4+}$ ($\text{Q} = \text{S or Se}$) complexes. The slope value of the plot observed for $[\{\text{Re}_6\text{Q}_6\text{Br}_2\}\text{Br}_6]^{2-}$ (slope = -4.9×10^{-3} and $r = 0.98$) is significantly larger than that observed for $[\{\text{Re}_6\text{Q}_8\}\text{X}_6]^{4-}$ (slope = -9.4×10^{-4} and $r = 0.95$). Equations 1 and 2 indicate that the slope value of an energy gap plot is determined by both the vibrational frequency inducing nonradiative decay ($h\omega$) and the vibrational displacement between the excited- and ground-states (S) as mentioned above. The larger slope value observed for the $\{\text{Re}_6\text{Q}_6\text{Br}_2\}^{4+}$ series as compared with that for $\{\text{Re}_6\text{Q}_8\}^{2+}$ thus indicates that the $\{\text{Re}_6\text{Q}_6\text{Br}_2\}^{4+}$ complexes should possess the smaller $h\omega$ and/or S value(s). Since the slope value observed for the $\{\text{Re}_6\text{Q}_6\text{Br}_2\}^{4+}$ complexes is almost 5 times larger than that for the $\{\text{Re}_6\text{Q}_8\}^{2+}$ series, eqs 1 and 2 will suggest that the smaller $h\omega$ value for $\{\text{Re}_6\text{Q}_6\text{Br}_2\}^{4+}$ as compared with that of $\{\text{Re}_6\text{Q}_8\}^{2+}$ could be the primary reason for the larger slope value in Figure 7. Provided the emissive excited-states of the

(99) Caspar, J. V.; Meyer, T. J. *J. Am. Chem. Soc.* **1983**, *105*, 5583–5590.

(100) Kitamura, N.; Ueda, Y.; Itoh, Y.; Yamada, K., unpublished results.

complexes being the core-centered excited-states, replacement of the $\{\text{Re}_6\text{Q}_8\}^{2+}$ core (Q = S (atomic number = 16) or Se (34) by two Br atoms (35) in $\{\text{Re}_6\text{Q}_6\text{Br}_2\}^{4+}$ (Q = S or Se) might be one of the reasons for the lower vibrational frequency inducing nonradiative decay in the $\{\text{Re}_6\text{Q}_6\text{Br}_2\}^{4+}$ complexes. At the present stage of the investigation, it is still unclear if the vibrational modes are responsible for the nonradiative decay. More detailed spectroscopic and photophysical studies on these chalcogenide-capped hexarhenium complexes including resonance Raman spectroscopy will elucidate further the excited-state properties of these complexes.

Conclusion

The chalcobromide-capped hexarhenium(III) complexes with terminal bromides ($[\{\text{Re}_6\text{Q}_{8-n}\text{Br}_n\}\text{Br}_6]^{n-4}$ (Q = S, Se) were prepared, and the complexes including the geometrical isomers of $[\{\text{Re}_6\text{Q}_6\text{Br}_2\}\text{Br}_6]^{2-}$ (Q = S, Se) were isolated by column chromatography. Characterizations of the complexes were conducted on the basis of ^{77}Se NMR, UV-vis absorption, photoemission/photophysical data as well as of the available data reported. All of the chalcobromide-capped complexes showed photoluminescence in both crystalline and solution phases at room temperature. It is worth noting that the replacement of one ~ three capped ligands in

the $\{\text{Re}_6\text{Q}_8\}^{2+}$ core by Br atoms gives rise to extension of the emission band to near-infrared ~ infrared region. This is the first observation of the entire emission spectra of the chalcobromide-capped hexarhenium(III) complexes in the 700–1400 nm range in both solid and solution phases. The emission maximum wavelength of the chalcobromide-capped complex shifted to the longer wavelength upon cooling from 296 to 80 K, which was the typical *T*-dependent emission characteristic for the hexanuclear complexes with 24 valence electrons. Owing to such photophysical properties, it was assigned that the photoemissive excited-state was of spin-triplet nature localized on the hexarhenium(III) core. The luminescence intensity of the complex was shown to become weaker when increasing the number of the Br atoms in the $\{\text{Re}_6\text{Q}_{8-n}\text{Br}_n\}^{n+2}$ core and lowering the symmetry of the $\{\text{Re}_6\text{Q}_{8-n}\text{Br}_n\}^{n+2}$ core. In addition to such photophysical characteristics of the complexes, the UV-vis absorption/emission spectra, emission quantum yield, and emission lifetime of the complex were shown to be the powerful means to identify the geometrical isomers of the complex.

Supporting Information Available: A figure of ^{77}Se NMR spectra, a figure of UV-vis absorption spectra, and figures of emission spectra. This material is available free of charge via the Internet at <http://pubs.acs.org>.